

## Research Paper

## A suction cup-based soft robotic gripper for cucumber harvesting: Design and validation

Yuseung Jo<sup>a,b</sup>, Yonghyun Park<sup>a,b</sup>, Hyoung Il Son<sup>a,b,c,\*</sup><sup>a</sup> Department of Convergence Biosystems Engineering, Chonnam National University, Yongbong-ro 77, Gwangju, 61186, Republic of Korea<sup>b</sup> Interdisciplinary Program in IT-Bio Convergence System, Chonnam National University, Yongbong-ro 77, Gwangju, 61186, Republic of Korea<sup>c</sup> Research Center for Biological Cybernetics, Chonnam National University, Yongbong-ro 77, Gwangju, 61186, Republic of Korea

## ARTICLE INFO

## Keywords:

Cucumber  
 Robotic harvesting  
 Grasping  
 Origami  
 Manipulator  
 End-effector

## ABSTRACT

The study introduces a suction cup-based soft robotic gripper for cucumber harvesting that adjusts its shape and surface parameters to respond to the surface and shape characteristics of cucumbers. The gripper shape is optimised for adsorption to the large curvature of the cucumber, increasing the effective radius related to the grasping force. The suction cup surface is also modified to maintain adsorption on uneven cucumber surfaces. The test of the suction cup verifies the validity of these critical parameters and demonstrates that the proposed gripper produces robust adsorption, increasing the adsorption success rate and effective radius. The gripper integrated with the cutting module was verified at three sites with varying cucumber characteristics. The test of the end-effector was conducted 174 times, and the success rate was 86.2%, with a damage rate of 4.7%. The success rate was lowest at Site A (76.8%) and highest at Site C (95.2%), which is attributed to the thickness and length of the cucumber stem. The gripper function is independent of the cutting module, and its analysis motivates the future improvement of the cutting module. The proposed gripper can contribute to effective cucumber harvesting when employed with the improved cutting module.

## 1. Introduction

Soft robotic grippers have been actively employed in the past decade, rapidly replacing rigid links in various applications, including industrial (Fontanelli et al., 2020), medical (Jang et al., 2021; Rateni et al., 2015), and agricultural (Blanes et al., 2015; Lee et al., 2020a; Low et al., 2021; Navas et al., 2021) applications. Because these applications deal with delicate or irregular objects, the traditional approach of using a robotic hand with multiple rigid fingers that mimic a human hand (Lange et al., 2021; Rahman et al., 2018) is no longer the most effective. Although robotic hands are designed to serve a universal purpose like the human hand, their high degree of freedom (DoF) and force requirements result in a large size and complex control (Cortés et al., 2017; Shafer & Deshpande, 2022; Zhu et al., 2023). In contrast, soft robotic grippers have a relatively low DoF. However, their task-specific design allows for an optimised grasping force with simple control, even when the gripper is quite small. The limitations of the traditional approach highlight the importance of soft robotics approaches. The small size and task-specific design of soft robotic-based grippers effectively address the limitations of the traditional approach. Therefore, soft robotic grippers address the

problem of maximising the grasping force with low control complexity in a small structure with flexible materials.

Soft grippers proficiently fulfil essential demand specifications in agricultural environments, encompassing a small size and soft materials. Most fruits and vegetables are grown in controlled environments to improve their marketability and yield (Wang et al., 2020). These environments are typically dense and atypical. In such environments, large end-effectors can cause collisions with nontargeted objects (e.g. leaves, stems, branches, and other fruits), leading to frequent control and perception errors (Blanes et al., 2015; Cao et al., 2019). These undesired contacts dramatically lower the perception and control accuracy for harvesting, significantly reducing the efficiency of the harvesting robots. In this agricultural environment, the compact and small size of the end-effector is a practical requirement. Particularly, cluster-grown fruits (e.g., tomatoes) and rod-shaped fruits (e.g., eggplant and cucumber) are sensitive to oscillation induced by undesired contact, which can reduce the harvest success rate.

Additionally, agricultural grippers must handle produce that often exhibits intricate or delicate characteristics. Soft robotic-based approaches have made rapid progress in addressing these challenges. These approaches are commonly used in many areas where objects with

\* Corresponding author. Yongbong-ro 77, Gwangju, 61186, Republic of Korea.

E-mail addresses: [chossbb68@jnu.ac.kr](mailto:chossbb68@jnu.ac.kr) (Y. Jo), [dk03378@jnu.ac.kr](mailto:dk03378@jnu.ac.kr) (Y. Park), [hison@jnu.ac.kr](mailto:hison@jnu.ac.kr) (H.I. Son).

Nomenclature			
$\tau$	Shear stress (kPa)	$F_{react}$	Reacting force by cutting (N)
$\vec{P}_0$	Suction contact vector (—)	$F_{z,max}$	Maximum grasping force (N)
$A$	Grasping area (mm <sup>2</sup> )	$k$	Curvature (—)
$a$	Major axis of the ellipse (mm)	$L_1$	Ideal contact perimeter (mm)
$b$	Minor axis of the ellipse (mm)	$L_2$	Ideal major axis of the ellipse (mm)
$c$	Hyperbolic constant (—)	$L_3$	Ideal minor axis of the ellipse (mm)
$e$	Eccentricity (—)	$L_{C(x,y)}$	Perimeter of an ellipse on plane (mm)
$E(e)$	Elliptic integral of the second kind (—)	$r$	Radius of cucumber (mm)
$F_{connected}$	Hanging force (N)	$r_{design}$	Ideal effective radius (mm)
$F_{gravity}$	Fruit weight (N)	$r_e$	Effective radius (mm)
$F_{holding}$	Grasping force (N)	$T$	Inertial torque (N mm)
		$V$	Pressure (kPa)

low stiffness or high complexity must be handled or targeted. Grippers using traditional rigid bodies can damage the fruit surface, severely degrading its marketability (Jang et al., 2021). Furthermore, large grippers can be challenging for practical applications because they could conflict with the surrounding environment (Wang et al., 2017). This study investigates the relationship between collisions of a finger-type gripper and nontargeted fruits during clustered tomato harvesting and evaluates the resulting harvest success rate (Rong et al., 2022). A grasping strategy was proposed to minimise collisions caused by other fruits in the cluster and determine the harvest order of clustered tomatoes. Although this strategy improved the success rate, collisions between neighbouring tomatoes and end-effectors remain a significant cause of failure. A gripper using a honeycomb structure was proposed as an application of soft robotics in agriculture, exhibiting highly sensitive grasping performance (Lee et al., 2020a). This gripper can grasp soft objects (e.g., paper cups and tofu), but its considerable idle state before grasping is a disadvantage for harvesting fruits growing in clusters. This paper proposes a suitable gripper for automating the harvesting of cucumbers, a representative cylindrical fruit embodying both of these challenges.

Research on grippers for grasping cucumbers has actively been conducted in the field of robotics. The simplest method for grasping is a parallel gripper (Guo et al., 2019; Li et al., 2013). Aoyama et al. (2022) performed research on picking and placing cucumbers for food packaging. The gripper designed in this study is a parallel gripper comprising two rigid fingers. A soft material was added to the fingers of the proposed gripper to prevent surface damage to the cucumber. However, this gripper presents challenges regarding direct application in harvesting because it is primarily designed for food packaging. Additionally, the gripper is large, which could cause excessive shaking of cucumbers due to collisions with the environment, which is detrimental to the harvest success rate. Moreover, collisions with cucumbers with a gripper that does not have the added soft material can cause surface damage.

Another common approach to preventing potential surface damage caused by rigid links is the use of soft actuators. Yang et al. (2022) proposed a gripper consisting of three soft fingers. Similar to the previously mentioned grippers, this gripper was primarily designed for picking and placing cucumbers for transportation, making it less suitable for harvesting. This gripper is constructed with soft materials to avoid damaging the cucumber surface, but problems related to its large size persist.

In another study involving soft actuators, Han et al. (2023) introduced a pneumatic soft actuator to create a gripper using multiples of such soft actuators to grasp cucumbers. Similarly, this research also highlights the relatively large size compared to the proposed gripper. Both of these grippers, based on soft actuators, have been assessed regarding the ability to grasp cucumbers. However, both the approach and grasping must co-occur in actual harvesting operations. Both

grippers have limited operating directions, restricting their versatility for various end-effector orientations.

Besides soft actuators (Alian et al., 2023; Liu et al., 2020; Lindenroth et al., 2023; Low et al., 2021), another representative grasping approach exists in soft robotics: suction (Fontanelli et al., 2020; Hayashi et al., 2011; Hudoklin et al., 2022; Jang et al., 2021; Navas et al., 2021). The suction cup-based approach has the advantage of a simple production process and relatively small size. However, grasping performance varies greatly depending on the surface of the grasping object, and an object-specific design is required for a curved surface. In other words, designing a gripper for harvesting fruits and vegetables is defined as the problem of minimising its size while satisfying the stiffness and grasping force requirements to avoid damaging the surface.

This study proposes a gripper design using a radius-maximised design and origami structure for atypical agricultural environments, specifically for harvesting cucumbers. As depicted in Fig. 1, two main challenges occur in grasping cucumbers with a suction cup regarding the large curvature of the cucumbers compared to spherical fruits and the bumpy and irregular surfaces of cucumbers that make it challenging to maintain attachment. The shape and surface of the suction cup, which are critical parameters in soft robotics, can be adjusted to address these challenges (Gilday et al., 2020; Yue et al., 2022). The proposed gripper has a conical shape projected onto the cucumber to accommodate its large curvature, and the origami structure on the surface improves the robustness of the attachment to the irregular cucumber surface. The hysteresis of the hyperelastic silicon material of the suction cup is maximised by the irregular surface conditions of the cucumber, which can decrease grasping performance. The origami structure serves as a deformation guide to minimise undesired deformation and maximise the adsorption area. Fig. 2 depicts the three-dimensional (3D) diagram of the proposed gripper, and Section 2 describes the detailed grasping challenges and designs.

### 1.1. Contribution and novelty

The contributions and novelty of this study are summarised as follows.

1. A soft, compact, small module that minimises collisions with atypical agricultural environments and does not cause damage to the fruit surface upon contact.
2. A radius-maximised design that corresponds to the large curvature of the cucumber cross-section by adjusting the shape of the suction cup and an origami structure that adjusts the surface of the suction cup to minimise undesirable deformation caused by the bumpy and irregular cucumber surfaces.
3. Experimental- and simulation-based grasping force and deformation analysis of the origami-inspired gripper.

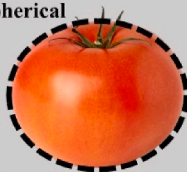
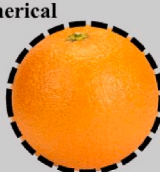
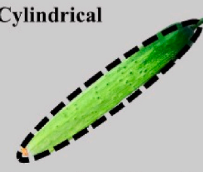



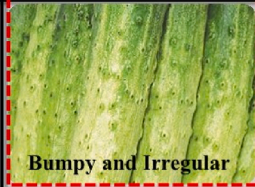

	Tomato	Orange	Cucumber	Eggplant
Shape of Fruit (curvature)	Spherical  ( $k = 0.24 \sim 0.32 [cm^{-1}]$ )	Spherical  ( $k = 0.24 \sim 0.33 [cm^{-1}]$ )	Cylindrical  ( $k = 0.54 \sim 0.8 [cm^{-1}]$ )	Cylindrical  ( $k = 0.4 \sim 0.57 [cm^{-1}]$ )
Surface of Fruit			 Bumpy and Irregular	

Fig. 1. Surface and shape characteristics of various crops, such as tomatoes, oranges, cucumbers, and eggplants. Cucumbers have shapes and surface features distinct from other fruits; thus, they require a soft robotic gripper specifically designed for them when grasping and cutting.

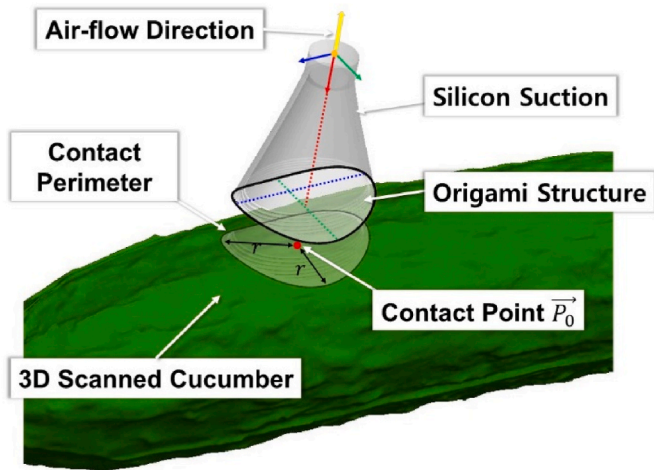


Fig. 2. Soft robotic gripper for cucumber harvesting with radius-maximised and origami-inspired designs. The elliptical grasping area and origami structure improve grasping on the bumpy and irregular cucumber surfaces.

4. Evaluation of the performance of the origami-inspired gripper through field evaluation. The evaluation is conducted in three commercialised cucumber farms which reveal the different shapes and surface characteristics.

## 2. Materials and methods

### 2.1. Design of the origami-inspired gripper

In most plants, the hierarchical structure consists of a stem connected to the root, a petiole (like a tree branch) connected to the stem, and a pedicel connected to the fruit on the petiole. Harvesting typically involves separating individual fruits from their pedicels. A human-centred approach mimicking the harvesting technique of human workers was chosen, as detailed in Fig. 3. The dual-arm harvesting method employed by human workers involves one arm cutting the pedicel and the other grasping the fruit. Harvesting is categorised into cutting and detaching operations, with the detaching operation further subdivided into picking, twisting, and plucking operations. However, detaching requires considerable force and may be unsuitable for soft fruits, depending on the fruit species, growth conditions, and pedicel width. Therefore, as depicted in Fig. 3(a), the cutting operation was chosen, similar to the

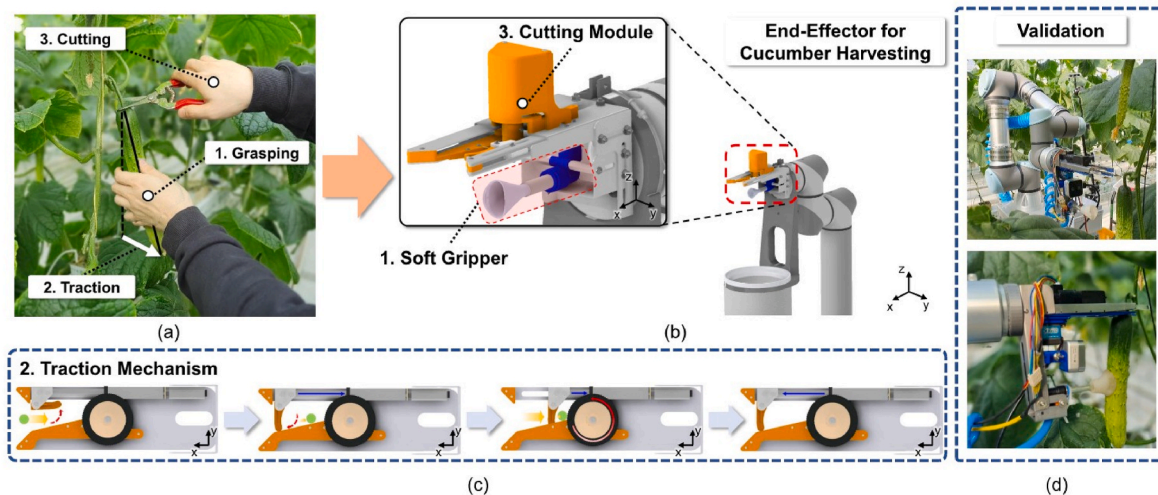


Fig. 3. Designed end-effector for harvesting robots. (a) The mechanism mimics a human harvesting method involving three subtasks: grasping, traction, and cutting. (b) The end-effector has cutting and grasping modules to replicate the human harvesting method. (c) The cutting module is used during traction operation. (d) The end-effector was been evaluated on commercial cucumbers in actual farms to verify its effectiveness.



manual harvesting method. Fig. 3(b) and (d) reveal the 3D model and real hardware of the end-effector. Moreover, Fig. 3(c) reveals the mechanism of the cutting module in the end-effector.

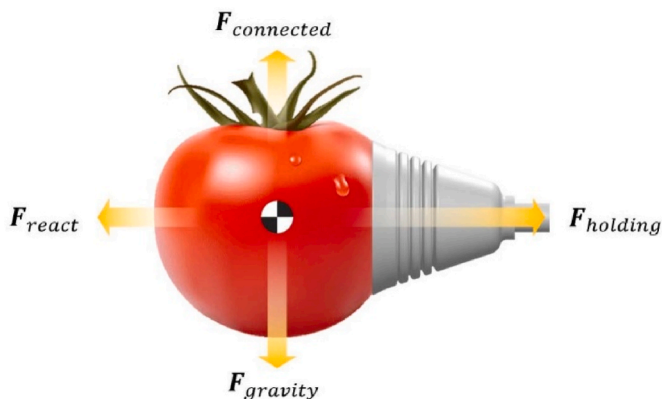
In robotic harvesting, cutting methods commonly involve scissors or circular saws. Previously, the authors introduced a scissor-type end effector in their study (Jun et al., 2021). However, its design, reliant on the reciprocating motion of the scissors, demands a larger workspace, which is impractical for dense harvesting environments. A subsequent study by the authors presented a circular saw-type end-effector to overcome

these limitations (Park et al., 2022). This design operates by rotating a circular saw through a simpler mechanism, substantially reducing the size of the end-effector. However, the circular saw must rotate at high speed to cut the fibrous pedicel, as illustrated in Fig. 4, where only the reactive force  $F_{react}$  caused by the saw rotation is considered, ignoring the gravitational force  $F_{gravity}$  on the fruit. In the human-centred approach, the grasping arm responds to the  $F_{react}$  generated by the cutting device. This reactive force induces pedicel bouncing, leading to undesired oscillations. These oscillations can negatively affect the harvesting success rate and perception accuracy, diminishing the efficiency of the robotic harvesting system.

The cucumber, which is the primary subject of this study, presents distinctive differences in shape and surface compared to spherical fruits and vegetables. Its elongated shape poses challenges in securing a firm grasp due to its narrow width. Additionally, the irregular and bumpy surface of the cucumber complicates maintaining a stable grasp against oscillation caused by cutting. These unique attributes render a conventional conical suction cup impractical. Hence, the proposed gripper was specifically designed to adjust its shape and surface characteristics to grasp the cucumber effectively.

#### 2.1.1. Shape: radius-maximised design

As discussed, the size of the end-effector is critical in a dense agricultural environment. The size of each module, including the cutting and grasping modules, must be minimised. Therefore, a circular saw-based cutting operation was selected that requires grasping to counteract the reaction force resulting from the rotational force. The performance of the suction cup is significantly influenced by its shape and material. When grasping soft-surfaced fruits and vegetables, silicone is a highly suitable material choice. Silicon offers the advantages of simple casting through 3D printed moulds and the flexibility to choose the stiffness level based on the fruit surface characteristics. Previous work demonstrated that silicon with a shore hardness of 5.0 does not damage soft fruits and vegetables (Jun et al., 2021). In this study, the proposed



**Fig. 4.** Relationship between the force on the fruit due to suction. A single fruit hangs from a pedicel and corresponds to its weight  $F_{gravity}$  by  $F_{connected}$ . In addition,  $F_{react}$  from cutting causes oscillation, reducing the perception accuracy and harvest success rate. Our previous study addressed  $F_{react}$  using a conical suction cup (Park et al., 2022).

grasping module uses the same hardness as silicon.

Several limitations of the conical grasping module in previous work were revealed for cucumbers. According to Eq. (1), the radius of the grasping area (the effective radius) is the most critical factor in the grasping force, and the grasping area must be sufficient to ensure the grasping force (Hudoklin et al., 2022):

$$F_{z,max} = r_e^2 \pi \Delta V, \quad (1)$$

where  $F_{z,max}$ ,  $r_e$ , and  $\Delta V$  represent the maximum pull-away load in the z-direction, the effective radius of the grasping area, and the pressure difference between the inside and outside of the suction cup, respectively. Due to the slight curvature of spherical fruit-vegetable cross-sections, an effective radius can be maintained in any adsorption direction. In contrast, as illustrated in Fig. 5, cucumber grasping scenarios have more limited grasping positions due to their larger cross-sectional curvature compared to spherical fruits.

Two solutions are proposed to address this problem: first, reducing the size of the suction cup, and second, adopting a cucumber-specific design. However, the first solution comes with an explicit limitation, as the grasping force also decreases as per Eq. (1). As illustrated in Fig. 5, this study selects a design that maximises the radius.

This design employs a hyperbolic paraboloid, as depicted in Fig. 6, which is a 3D surface characterised by two intersecting families of straight lines, creating a hyperbolic shape. One distinctive feature of a hyperbolic paraboloid is its double curvature, resembling a saddle or the shape of specific architectural structures, such as hyperbolic paraboloid roofs. The mathematical definition of the hyperbolic paraboloid is provided in Eqs. (2) and (3):

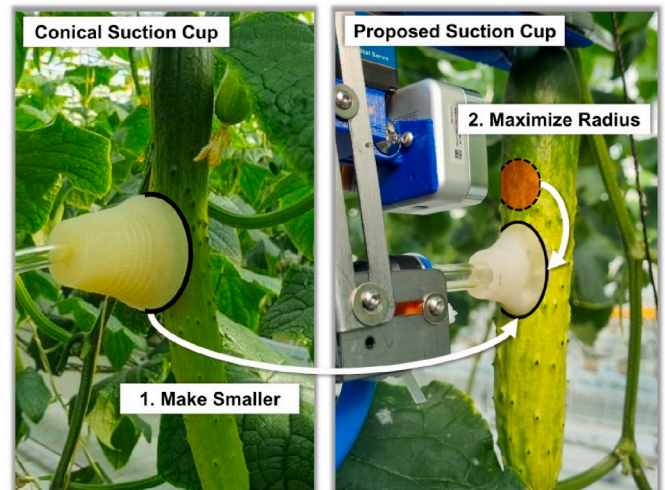
$$\frac{z}{c} = \frac{x^2}{a^2} - \frac{y^2}{b^2}, \quad (2)$$

$$\frac{x^2}{a^2} + \frac{y^2}{b^2} \leq 1. \quad (3)$$

When a hyperbolic paraboloid is used for the suction cup, the grasping area is defined as an ellipse, as indicated in Eq. (4).

$$\frac{x^2}{a^2} + \frac{y^2}{b^2} = 1, \quad (4)$$

where  $a$  and  $b$  represent the lengths of the major and minor axes of the



**Fig. 5.** Shape: Direction of improvement of the suction cup for effective cucumber grasping. By making the radius smaller, the effective radius associated with the adsorption force is reduced, and a sufficient grasping force is not obtained. A radius-maximised design is applied to the suction cup to solve this problem.



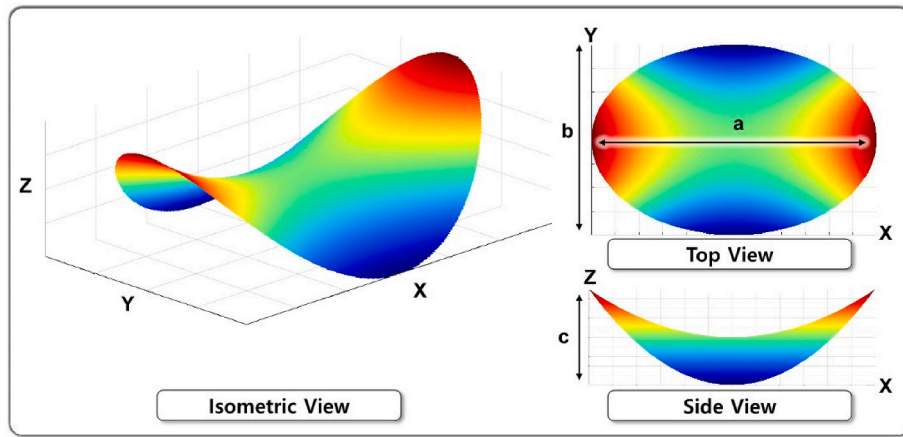


Fig. 6. Example of hyperbolic paraboloids:  $a$ ,  $b$ , and  $c$  are the parameter values of the hyperbolic paraboloid [in millimetres].

ellipse in the top view of Fig. 6, respectively. The variable  $c$  corresponds to the scale factor of the surface and is responsible for expanding or contracting the surface along the  $z$ -axis, influencing the overall shape and size of the surface. Typically,  $c$  serves as a parameter to adjust the surface height. Modifying the value of  $c$  results in changes in the geometric characteristics of the hyperbolic paraboloid.

The suction cup relies on the pressure difference between the inside and outside to grip the object. Thus, the structure must withstand deformation during grasping and should secure a circular grasping area to prevent deformation from interfering with the grasping process. Using an ellipse and hyperbolic paraboloid is the most effective approach to ensuring an adequate grasping area for thin and elongated cucumbers.

The proposed is designed based on measurements of the thickness of commercially available cucumbers. The initial step in crafting the suction cup involves accounting for the lateral thickness of cucumbers. The widths of 10 commercially available cucumbers were measured, and the average of the thickest was 37 mm, whereas the average of the thinnest was 25 mm. No absolute standards exist for the angles and heights at which cucumbers should be grasped and cut; thus, this study considers a thickness of the suction cup (1.6 mm) not exceeding the minimum cucumber thickness of 25 mm.

In Eqs. (2)–(4), the values for  $a$  and  $b$  are 14 and 10, respectively. Based on the defined attachment area, a suction cup was devised consisting of an ellipse, as described in Eq. (4), along with a circular region with a diameter matching that of a 10 mm rubber hose.

The next step involves determining the scale factor, denoted as  $c$ . As mentioned, this scale factor significantly influences the geometric properties of the hyperbolic paraboloid. As each agricultural product is unique and cannot be generalised, a similar approach to determining an ellipse can be used. The cucumber curvature can be calculated using commercially available cucumbers as a reference. When the cucumber radius is  $r$ , the curvature  $k$  is defined as indicated in Eq. (5):

$$k = \frac{1}{r}. \quad (5)$$

As depicted in Fig. 1, the curvature of commercially available cucumbers falls within the range of  $0.54\text{--}0.8\text{ cm}^{-1}$ . The surface of a cucumber can be modelled as a circle (defined in Eq. (6)) using the curvature  $k$ :

$$x^2 + y^2 = \frac{1}{k^2}. \quad (6)$$

The  $y$  and  $z$  coordinates of the contact points between the hyperbolic paraboloid and cucumber cross-section determine the value of  $c$ , as represented by Eq. (6). These coordinates are given by  $(-y_{\text{circle}}, z_{\text{circle}})$  and  $(y_{\text{circle}}, z_{\text{circle}})$ . In this case, the value of  $c$  is defined in Eq. (7):

$$c = r - z_{\text{circle}}. \quad (7)$$

As part of the design to accommodate irregular agricultural produce, a minimum curvature of  $k = 0.8\text{ cm}^{-1}$  is selected. In this case, the radius is 1.25 cm. In this scenario, the values of  $y_{\text{circle}}$  and  $z_{\text{circle}}$  are 1 and 0.5, respectively. The scale factor  $c$  is 0.75.

### 2.1.2. Surface: origami-inspired design

Grasping cucumbers poses a significant challenge owing to their elongated, thin shape with pronounced curvature in the cross-section. Furthermore, their uneven and bumpy surfaces lead to unpredictable deformations of suction cups, making grip retention challenging. The restriction in using conical suction cups primarily arises from the unique shape of the cucumber, a challenge partially addressed through a radius-maximised design. However, the current suction cup design fails to resolve the problem of coping with an irregular surface.

Silicon deformation induces hysteresis, where the system state heavily relies on the deformation history of the material. Dealing with irregular surfaces exacerbates this, resulting in an unstable initial contact between the suction cup and cucumber. This instability, stemming from unpredictable cucumber surface characteristics, significantly affects grasping performance due to deformation hysteresis. We propose an origami-inspired structure to mitigate these challenges. Origami, a compound word comprising ‘ori’ (folding) and ‘gami’ (paper), is a type of art in Japanese culture. Origami has recently gained attention in robotics for space-saving and changing structures based on external forces (Lee, Wang, & Zheng, 2020; Li et al., 2019).

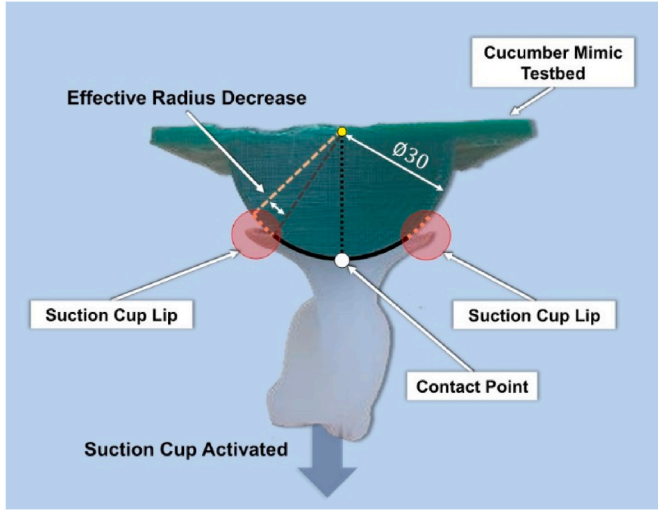
The origami structure empowers the design process to dictate folding and bending directions, a promising solution for effective cucumber grasping. Fig. 7 illustrates instances in which the suction cup lip fails to sustain a grasp (Lubbers et al., 2022). Therefore, in the design process, the deformation direction was predefined by inserting micro-etchings into the inner space of the suction cup lip, which can minimise undesired deformation due to the irregular surface. The detailed design parameter is depicted in Fig. 8.

## 2.2. Analysis of the origami-inspired gripper

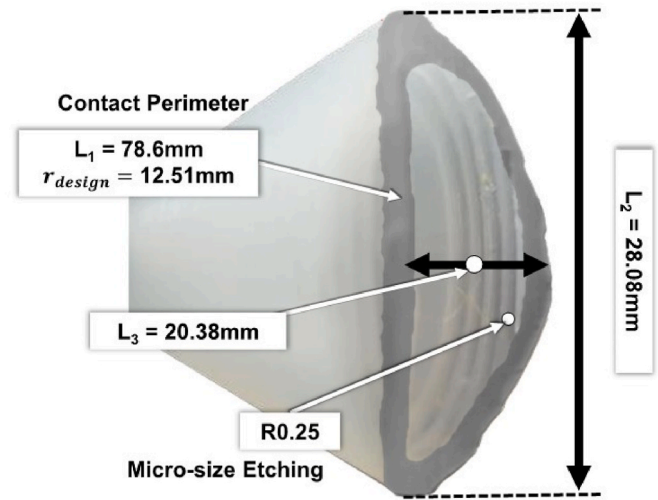
### 2.2.1. Grasping force analysis of the suction cup

Definitions must be established for the grasping area and contact perimeter, representing the perimeter of the grasping area, to analyse the grasping force of the proposed suction cup. The grasping area is defined in Eq. (4). The contact perimeter consists of points on a 3D cucumber with a geodesic distance of  $r$  from the contact point  $P_0$ . Consequently, the contact perimeter is defined in Eq. (8):

$$C = \left\{ P(x, y, z) \mid (x - x_{P_0})^2 + (y - y_{P_0})^2 + (z - z_{P_0})^2 = r_e^2 \right\}, \quad (8)$$



**Fig. 7.** Surface: In the gripper, which only adjusts the shape, adsorption did not occur in the suction cup lip when the suction cup was activated and deformed. Incomplete adsorption reduces the effective radius and is observed more extremely in the bumpy surface of cucumbers. Employing the origami structure as a suction cup deformation guide solves the problem.



**Fig. 8.** Detailed design specification. The grasping area of the gripper is the same as the ellipse composed of  $L_2$  and  $L_3$ . Inside the suction cup, several micro-size etchings of R0.25 exist without intervals. Due to this structure, the gripper folds in the desired direction. In addition,  $L_1$  is the contact perimeter of the suction cup and  $r_{design}$  is the ideal effective radius derived using the previous specification.

where  $r_e$  represents the effective radius of the suction cup, and  $x_{P_0}$ ,  $y_{P_0}$ , and  $z_{P_0}$  denote the  $x$ ,  $y$ , and  $z$  coordinates, respectively, of the contact point  $P_0$ . Notably,  $P(x, y, z)$  consists solely of points on the cucumber surface. The effective radius, derived from Eq. (1), is defined by Eq. (9):

$$r_e = \sqrt{\frac{F_{z,max}}{\Delta V \pi}}, \quad (9)$$

where  $r_e$  is a measurement value derived from  $F_{z,max}$ , which is a measurement of the maximum pull-away load of the suction cup.

Employing a hyperbolic paraboloid-based radius-maximised design reveals that the adsorption area for cucumbers is in the shape of the ellipse defined in Eq. (4). The length  $L_{C(x,y)}$  of the contact perimeter in the  $xy$  plane can be calculated using Eqs. (4) and (10):

$$L_{C(x,y)} = 4aE(e), \quad (10)$$

where  $E(e)$  is defined in Eq. (11) by an elliptic integral of the second kind:

$$E(e) = \int_0^{\frac{\pi}{2}} \sqrt{1 - e^2 \sin^2 \theta} d\theta, \quad (11)$$

where  $e$  denotes the eccentricity of the ellipse and is defined in Eq. (12):

$$e = \sqrt{1 - \left(\frac{b^2}{a^2}\right)}. \quad (12)$$

For the quantitative evaluation of the grasping force of the proposed suction cup, the calculated perimeter of the ellipse can be converted into a circle with an ideal effective radius  $r_{e,ideal}$ . In this case,  $r_{e,ideal}$  is calculated in Eq. (13) using the circumference equation of a circle:

$$r_{e,ideal} = \frac{L_{C(x,y)}}{2\pi}. \quad (13)$$

As depicted in Fig. 8, the calculated ideal contact perimeter  $L_{C(x,y)}$  is 78.6 mm and the effective radius  $r_{e,ideal}$  is 12.51 mm. The actual effective radius of Eq. (9) can be experimentally calculated, and these values can be compared with the calculated ideal effective radius to evaluate the adsorption effectiveness of the proposed suction cup. A test of the suction cup was conducted to measure the experimental variables, pull-away load, and pressure difference.

#### 2.2.2. Deformation analysis of the suction cup

Silicone is a hyperelastic material; thus, powerful grasping on the surface by a suction cup causes high torsion (Valiollahi et al., 2019), which acts on a small area of the suction cup and appears as a deformation of the suction cup. The effectiveness of the design is verified by checking the vacuum sealing ability of the proposed suction cup on uneven surfaces.

For verification, a simulation-based finite-element analysis was performed. As illustrated in Fig. 9, the presence or absence of an origami structure was set as an experimental variable for verification. As an experimental scenario, the experiment begins with suction on an uneven surface, simulating the cucumber surface and applying a pull-away load to the suction cup. The evaluation was performed using deformation.

Table 1 lists the verification results, indicating that about 1.326–1.350 times higher deformation occurred.

on surfaces with uneven origami structures. These results indicate that a suction cup with an origami structure is more robust against irregular and bumpy surfaces than a suction cup without an origami structure.

However, the simulation-based micro-area approach may vary due to the hysteresis in analysing the interaction between the suction cup and real-world objects. In the field of basic static structural analysis, the torsion is simplified, as defined in Eq. (14) (Horgan & Saccomandi, 1999):

$$T = \int \tau r dA. \quad (14)$$

The inertial torque is assumed to equal the sum of the moments of the  $x$ -,  $y$ -, and  $z$ -axes, as indicated in Eq. (15). In this study, the validity of the origami structure is verified using Eq. (15):

$$T = M_x + M_y + M_z. \quad (15)$$

The real-world validation of the deformation was conducted in the test of end-effector at three different commercial cucumber farms.

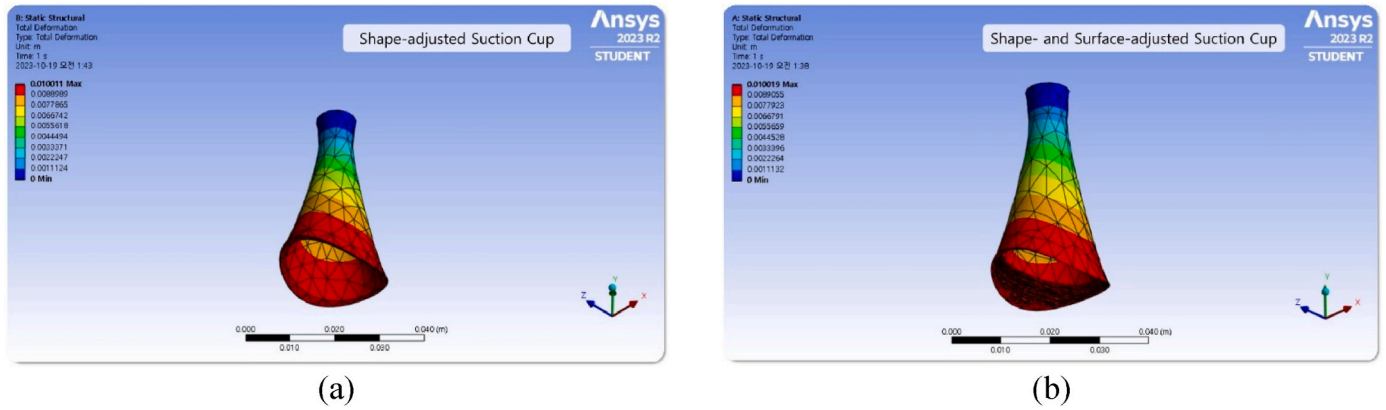


Fig. 9. Simulation-based finite-element analysis of the suction cup deformation. (a) shape-adjusted suction cup, (b) shape- and surface-adjusted suction cup.

**Table 1**  
Deformation analysis results.

Deformation	Shape-adjusted			Shape- and surface-adjusted		
Time (s)	Minimum (m)	Maximum (m)	Average (m)	Minimum (m)	Maximum (m)	Average (m)
0.2	0.	2.0036e-003	1.3433e-003	0.	2.0079e-003	1.8130e-003
0.4	0.	4.0064e-003	2.7036e-003	0.	4.0130e-003	3.6269e-003
0.7	0.	7.0092e-003	4.7894e-003	0.	7.0171e-003	6.3652e-003
1	0.	1.0011e-002	6.8624e-003	0.	1.0019e-002	9.1029e-003

## 2.3. Experimental design

### 2.3.1. Experimental design of the test of suction cup

In the real world, Eqs. (9) and (13) verify the performance of the proposed suction cup. The essential variable in these formulas is the 6 DoF grasping force of the suction cup. The 6 DoF force of the proposed suction cups was measured in a laboratory environment to validate them. Fig. 10 depicts the detailed experimental setup. The experimental environment consists of two manipulators. One manipulator with a

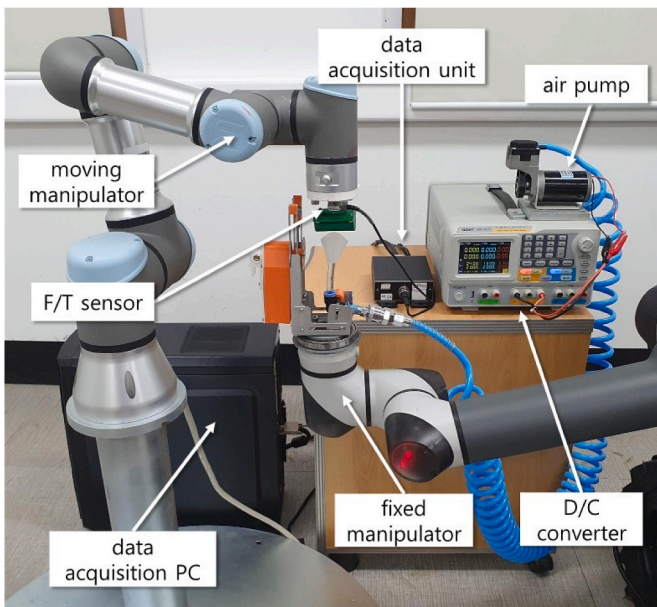


Fig. 10. Experimental setup of the suction cup test. The experiment was performed using two manipulators for easy reproduction and repetition. The fixed manipulator has a testbed mimicking a cucumber and a 6 DoF force sensor. The moving manipulator is equipped with an end-effector using grippers from our previous work, including the proposed gripper. The experiment repeats the process of entry, adsorption, and desorption using the moving manipulator.

constant pose is equipped with a grasping testbed with a diameter of 30 mm (mimicking the thickness and curvature of cucumbers) and an ATI Nano17 6 DoF force sensor. The other manipulator comprises the cutting module depicted in Fig. 3 and the proposed gripper. The moving manipulator has the same x- and y-coordinates as the fixed manipulator, moving only on the z-axis in the height direction. In this experiment, the grippers consist of three suction cups: (1) our previous suction cup (i.e., a conical suction cup), (2) the shape-only-adjusted suction cup, and (3) shape- and surface-adjusted suction cups. In this experiment, the gripper is connected to an air pump with a vacuum force of 620 mmHg.

The experimental procedure is described below.

- Step A: The moving manipulator moves to the initial pose, the initial end-effector pose of the moving manipulator, which is only a z-coordinate different from the end-effector pose of the fixed manipulator.
- Step B: The vacuum pump operates.
- Step C: The moving manipulator moves to the desired pose, the desired end-effector pose of the moving manipulator, which is the same as the end-effector pose of the fixed manipulator.
- Step D: A steady state of grasping is reached.
- Step E: The moving manipulator moves to the initial pose.

During this process, the grasping of the suction cup is conducted in Step C, and the steady state of attachment in Step D is adequately verified with sufficient time to be visually confirmed before proceeding to the next step. In this case, a failure is defined as a case without grasping, and no further process is performed. Step E focuses on the maximum absolute value, which is the yield point. The experiment was repeated 10 times for each gripper.

### 2.3.2. Experimental design of the test of end-effector

The performance of the proposed gripper was evaluated in the test of suction cup. However, as illustrated in Fig. 3, the gripper is one end-effector component. As discussed in Section 2, the gripper is attached to the end effector for stable cutting during harvesting. Therefore, the evaluation of soft robotic grippers should be integrated with the cutting module as the end-effector.



The test of end-effector was conducted in three environments with varying pedicel thicknesses and fruit lengths, shapes, and surfaces to verify the cutting and grasping modules rigorously. Sites A, B, and C, where the test of end-effector was conducted, are greenhouses in Boryeong, Sangju, and Cheongju City in Korea, respectively. The test of end-effector was performed using the mobile manipulator platform illustrated in Fig. 11.

As revealed in Fig. 12, the experimental procedure is described below.

- Step 1: Position the mobile platform for the cucumbers to be harvested. At this point,  $p_{initial}$ , the end-effector pose, is random.
- Step 2: Determine the position of the waypoint  $p_{waypoint}$  just before approaching the cucumber. In Eq. (16),  $p_{waypoint}$  is defined based on the centre point of the  $p_{cucumber}$ . In addition,  $p_{waypoint}$  is sufficiently far from  $p_{cucumber}$  to prevent collisions with other cucumbers:

$$p_{waypoint} = p_{cucumber} + p_{offset}, \quad (16)$$

where  $p_{offset} = (0, 150, 150)$  [mm].

- Step 3: Approach the end-effector from  $p_{waypoint}$  to  $p_{destination}$ , where  $p_{destination}$  denotes the appropriate pedicel cutting point. In addition,  $p_{destination}$  is defined based on the average pedicel

length of marketable cucumbers after cutting.

- Step 4: The arrival at  $p_{destination}$  signifies that the pedicel is positioned within the cutting area of the end-effector. The vacuum pump is activated in this process, and the cutting unit in the end-effector performs the cutting.

As displayed in Fig. 13, despite the atypical shape of the cucumbers, their high weight and thin pedicel cause them to align perpendicularly to the ground. Therefore, a simple entry along the approach vector consistent with the y-axis in the replication can maintain the same entry angle of the end-effector. The performance metrics include quantitative and qualitative results. In the experiment, the harvest success rate is measured as a quantitative metric, whereas the number of fruits with damaged surfaces is measured as a qualitative metric.

### 3. Results

#### 3.1. Result of the test of suction cup

The experimental results of the suction cup test are depicted in

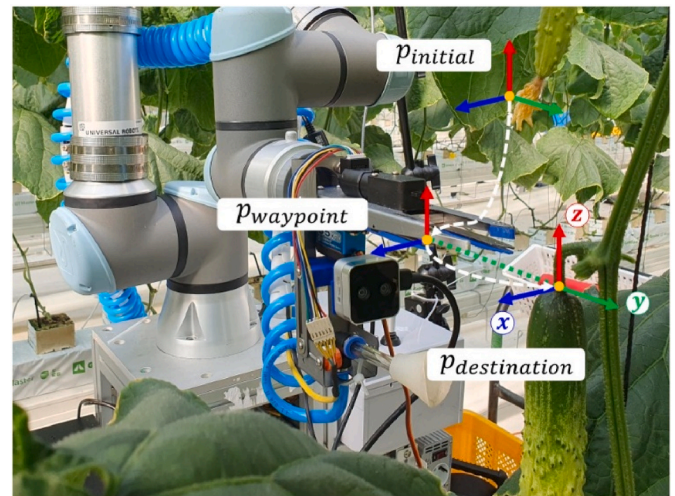


Fig. 12. Second experimental procedure:  $p_{initial}$  is the random initial position of the robotic system, and  $p_{waypoint}$  matches the coordinate of the cucumber and the x- and z-coordinates. A robot that reaches  $p_{waypoint}$  moves along the y-axis approach vector.

Fig. 14. In the cucumber testbed, the conical suction cup was not attached; thus, no data were observed. In contrast, both grippers exhibited a 100% success rate in the shape-adjusted suction cup and shape- and surface-adjusted suction cup. The experimental procedures and results are detailed in Figs. 15 and 16 for one of the 10 cases. As depicted in Fig. 15, the average pull-away load of the shape-adjusted gripper is 6.660 N, and the shape- and surface-adjusted gripper has an average pull-away load of 2.253 N. The resulting values of the 10 repetitions were statistically analysed using a *t*-test, confirming that the significance probability was under 0.001 ( $\alpha = 0.05$ ). Thus, the pull-away load difference between the two suction cups was significant.

In addition, according to Eq. (9), the effective radius  $r_{shape}$  of the shape-adjusted gripper is 6.2109 mm, and the effective radius  $r_{both}$  of the proposed gripper is 10.6616 mm. The contact perimeter  $L_1$  of the ideal suction cup in Fig. 8 is 78.6 mm, where the attachment area is elliptical. The method in Eq. (13) can be used to determine the ideal effective radius of a suction cup, assuming the attachment area is a circle. The  $r_{ideal}$  derived by Eq. (13) is 12.51 mm. In conclusion, compared to the ideal suction cup, the shape-adjusted gripper confirmed a 49.6% effective radius, and the shape- and surface-adjusted gripper confirmed an 85.2% effective radius.

The torsion results for the suction cup in Fig. 16 were evaluated using

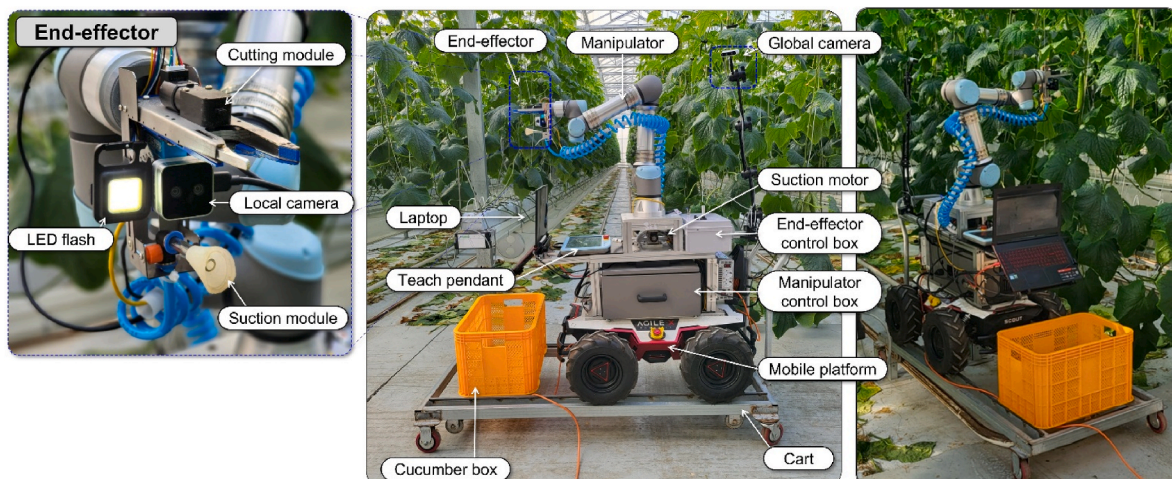
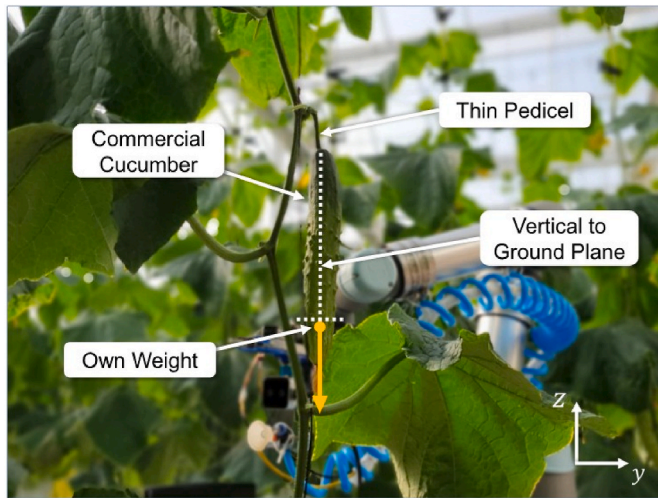


Fig. 11. Robotic harvesting platform details for the experiment (Park et al., 2023).



**Fig. 13.** Cucumber aligned vertically to the floor. Commercially available cucumbers are perpendicularly aligned to the floor due to their heavier weight compared to the thin pedicel, and these conditions indicate that no significant adjustment to the angle of entry in the repetition is needed.

Eq. (15). Unlike the pull-away load, high torsion can be used to evaluate whether the grasping can remain robust when the suction cup is deformed and twisted. The performance in scenarios where the suction cup is attached to the cucumber and deformed on bumpy and irregular surfaces was evaluated using the torsion results. The results reveal that the torsion  $T_{shape}$  of the shape-adjusted gripper was 37.68 Nmm, and the torsion  $T_{both}$  of the shape- and surface-adjusted gripper was 71.26 Nmm. Additionally, the *t*-test confirmed that the difference between the two grippers is significant.

In summary, the experiment was conducted to assess three aspects: the possibility of grasping a cucumber on a mimic testbed, the ability to grasp cucumbers with a large curvature, and the robustness of grasping bumpy and irregular cucumber surfaces. The results indicate that conical suction cups are unsuitable, with a 0% success rate in cucumber attachment scenarios. Additionally, when comparing the shape-adjusted gripper with the shape- and surface-adjusted gripper, the proposed gripper exhibits robust grasping for cucumbers with large curvatures and uneven surfaces.

### 3.2. Result of the test of end-effector

Table 2 presents the results of the test of end-effector. A total of 174 individual cucumbers were harvested, with 150 successes and 24

failures recorded. In addition, seven instances of surface damage were observed on the cucumbers. In this context, harvest success refers to the situation in which a single fruit is completely separated from the petiole through the rotation of a circular saw. It does not include cases where the fruit falls freely due to its weight when the saw fails to cut completely. Surface damage refers to scratches on the fruit, even after harvest. The overall success rate was 86.2%.

The experiment evaluated the effectiveness of the end-effector in various cucumber farm environments with varying pedicel thicknesses, fruit sizes, and surface characteristics. The success rates for Sites A, B, and C were 76.8%, 93.1%, and 95.2%, respectively. The highest success rate was recorded at Site C (95.2%), whereas the lowest was at Site A (76.8%). Seven instances (4.7%) of fruit damage were confirmed, with three at Site A (4.8%), two at Site B (7.4%), and two at Site C (3.3%). The site with the highest damage rate was Site B (7.4%).

## 4. Discussion

### 4.1. Pump-actuated suction cup

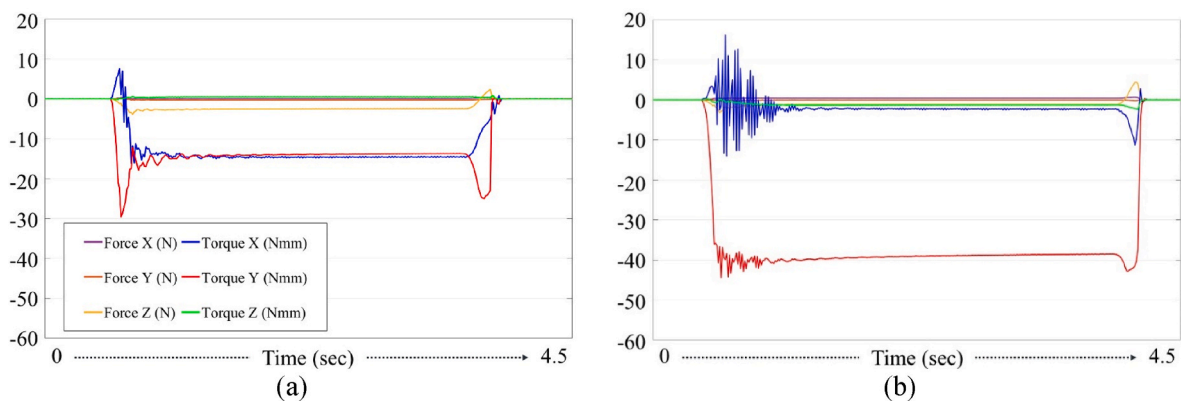
In the design process, determining the power source of the suction cup is a critical problem. There are two options:

- Method 1: Generate and adsorb the internal vacuum through suction cup compression.
- Method 2: Use an external vacuum source (e.g., an air pump).

After implementing the proposed suction cup, both methods could grasp the cucumbers. However, Method 1 had a higher frequency of failure to maintain adhesion to the bumpy surface of cucumbers than Method 2. The rotation of the yaw angle of the cucumber primarily caused the failure in Method 1. In contrast, Method 2 exhibited a stronger grasping force based on a stronger external vacuum source and was relatively more robust against the yaw rotation of the cucumbers. The circular saw of the cutting module frequently rotates, causing yaw angle rotation; thus, Method 2 is more effective in achieving more stable cutting success.

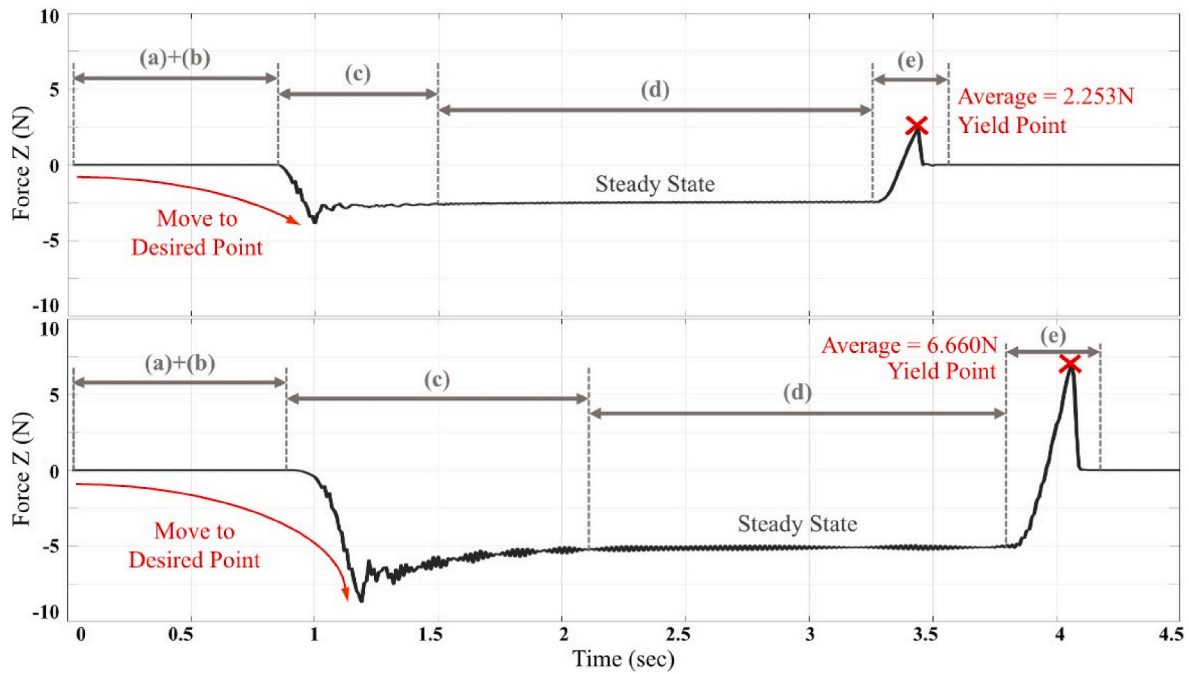
### 4.2. Unusual success reduction: Site A

The test of end-effector was conducted at three sites with varying environmental conditions to evaluate the performance of the end-effector. The results revealed that Site A had the lowest harvest success rate compared to Sites B and C. As depicted in Fig. 17, Site A (i.e., green monsters) had a thicker pedicel with a length of up to 15 mm shorter than the other sites. In addition, Table 2 demonstrates that the thickness of the pedicel is closely related to the harvest success rate. The

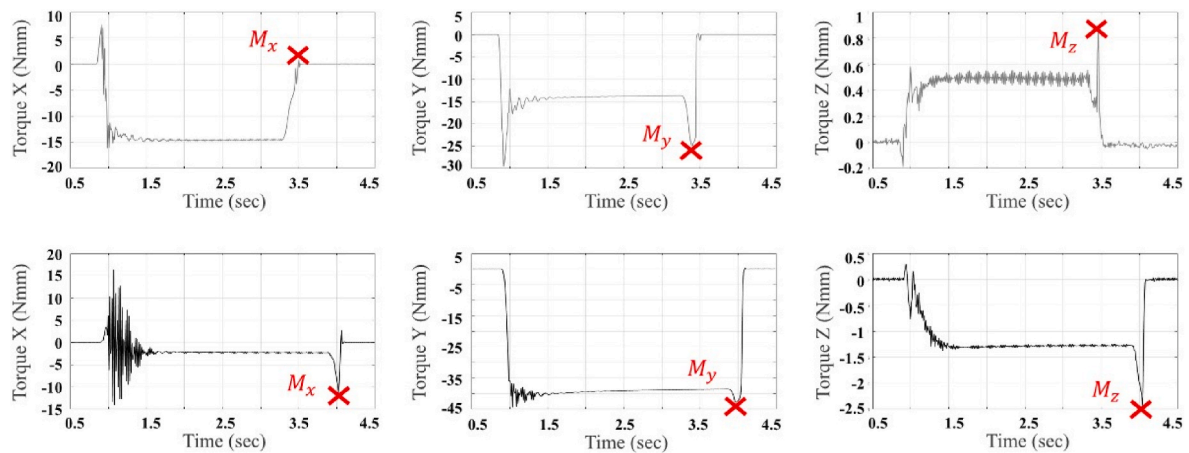


**Fig. 14.** Experimental results of the suction cup test. Only two types of gripper data exist because the conical suction cup in our previous study had a grasping success rate of 0%. Each figure represents only 1 out of 10 repetitions. Force and torque results of the soft robotic gripper with (a) only the shape adjusted and (b) both the shape and surface adjusted.





**Fig. 15.** Force  $F_z$  results in the  $z$ -direction (the pull-away load) and the experimental process of the soft robotic gripper with (top) only the shape-adjusted and (bottom) both the shape- and surface-adjusted (Case #6).



**Fig. 16.** Torque measurement results of the soft robotic gripper with (top) only the shape-adjusted and (bottom) both the shape and surface-adjusted:  $M_x$ ,  $M_y$ , and  $M_z$  (Case #6).

**Table 2**

Results of the test of end-effector in various fields.

Sites	Metric		Damaged
Site A	Success rate (%)	76.8% (63/82)	4.8% (3/63)
Site B	Success rate (%)	93.1% (27/29)	7.4% (2/27)
Site C	Success rate (%)	95.2% (60/63)	3.3% (2/60)
Total	Success rate (%)	86.2% (150/174)	4.7% (7/150)

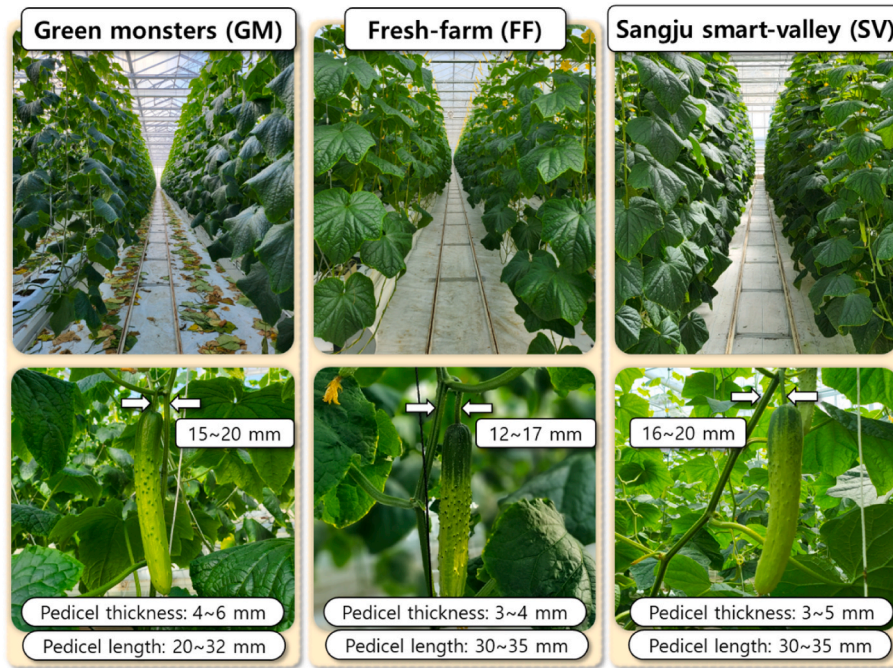
primary cause of harvest failure was the incomplete cutting of the thin fibres of the stem within 1 mm, resulting in the fruit not being separated or dropping due to its weight. This decreasing tendency aligns with the tendency in pedicel thickness depicted in Fig. 17. Fig. 18 illustrates the cause of the significant harvest failure and its analysis.

As revealed in the results of the test of end-effector, especially at Sites B and C, the high success rate indicates that these failure cases are aberrant (93.1% and 95.2%, respectively). Although, the necessity of the

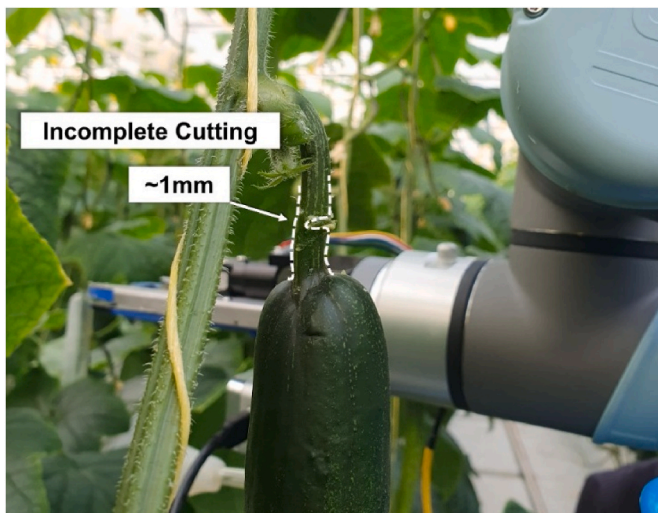
end-effector is remaining. As depicted in Fig. 19, another problem occurred in the approaching phase of the end-effector, movement between  $p_{waypoint}$  and  $p_{destination}$ . In Fig. 19(a)—a case was observed where the space between the stems and pedicel was not sufficient to fit the entrance of the cutting module of the end-effector. In addition, in Fig. 19 (b), even after entering  $p_{destination}$ , the fruit neck could not be cut because it was caught in the cutting unit of the end-effector. This situation occurs due to the large cutting module. Furthermore, this point highlights the importance of miniaturisation of the cutting modules in future research. Currently, we plan future work to miniaturise the cutting module.

Improvements to the cutting module are ongoing to address the problem of incompletely cutting the fibrous pedicel. These improvements include (a) increasing the traction range of the traction mechanism to bring the pedicel closer to the circular saw, (b) increasing the diameter of the circular saw for greater versatility, (c) establishing a visual or sensory system capable of detecting incomplete cutting to perform recutting, and (d) making the end-effector smaller and more





**Fig. 17.** Three different pedicel thickness and pedicel length characteristics of each size. Site A represents green monsters, Site B represents fresh-farm, and Site C represents Sanju smart-valley (Park et al., 2023).



**Fig. 18.** Incompletely cut cucumber pedicel, with an average of 1 mm of incomplete cutting.

compact.

#### 4.3. Determining $p_{\text{waypoint}}$ , $p_{\text{cucumber}}$ , and $p_{\text{destination}}$

This paper contributes to developing an autonomous cucumber harvesting robot (Park et al., 2023). Autonomous cucumber harvesting robotic platforms are configured in progress (in the test of end-effector) that can perform (1) deep neural network-based cucumber object detection and localisation (approach from  $p_{\text{initial}}$  to  $p_{\text{waypoint}}$ ), (2) computer vision-based cutting-point decision algorithms to determine, and (3) a 6-DoF position-based visual servoing algorithm that can accurately approach the cutting area in real-time despite shaking cucumbers (from  $p_{\text{waypoint}}$  to  $p_{\text{destination}}$ ). We plan to evolve the system into a universal fruit and vegetable harvesting robot through the analysis and development of a wider range of fruits.

#### 4.4. Comparison with the state-of-the-art methods

Compared to the existing cucumber grippers, the proposed gripper has some advantages (Aoyama et al., 2022; Han et al., 2023; Yang et al., 2022). These studies do not focus on the harvesting task, just on picking and placing cucumbers. Focusing only on the harvesting task has advantages, such as the compact size of the soft gripper, an unrestrained entry pose, and the ease of manufacturing and replacement.

Unlike parallel and finger-type grippers that use multiple fingers, the proposed gripper is a single module with a suction cup powered using a rubber hose. This configuration satisfies the specifications for cucumber grasping and enables maximum miniaturisation. Notably, grippers comprising rigid links may pack soft material on the contact surface of the fruit, and in this case, the gripper becomes thicker. Additionally, control and recognition errors in the harvest robot can cause the gripper to collide with the fruit. In this case, a gripper consisting of a rigid link packed with soft material may damage the fruit surface due to collision. However, the proposed gripper is entirely constructed of soft material; therefore, there is no possibility of damaging the fruit during grasping or collision.

The proposed gripper has no limitations on the entry angle for grasping the fruit. The cylindrical fruit standing against the ground has morphological characteristics that allow it to be gripped from any entry angle. However, the finger-based gripper has a limited entry angle depending on the DoFs and workspace. However, the proposed gripper was designed to grasp most cylindrical fruits. Therefore, the gripper has an advantage in grasping cylindrical primitives in most situations.

Most diseases in agriculture are contagious (Orzali et al., 2017; Mahlein, 2016; Barbedo, 2016; Oberti et al., 2016), and disease spreading during harvesting causes fruit trees to wilt, resulting in significant losses to farmers because harvesting can no longer be performed. Therefore, low cost, easy manufacturing, and numerous replacements are clear advantages in agriculture. However, this problem has not been considered for other grippers, and because they are expensive, repeated replacement causes a loss in economic efficiency.

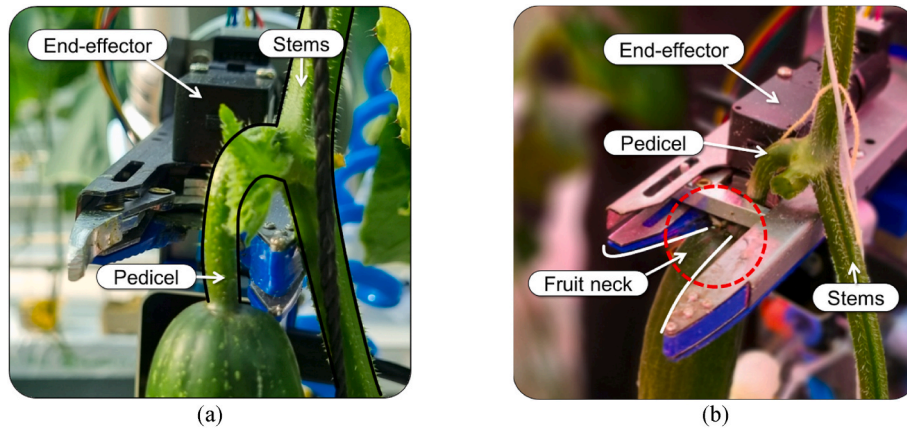


Fig. 19. Cutting failure cases in the test of end-effector: (a) narrow space, (b) large cutting module (Park et al., 2023).

#### 4.5. Success rate-based experiment: Relationship to suction

The primary evaluation metric during end-effector testing was the cutting success rate, rather than the suction grasping success rate. The soft gripper proved effective as a complementary component of the end-effector to counteract the reaction force of the circular saw. Its design provided robust adsorption power for cucumber, leveraging torsion for an optimised effective radius and elliptical adsorption area. This enhanced adsorption force adeptly managed the reaction force of the circular saw within the cutting module. The relatively low failure rate of 24 out of 174 cases indirectly validates the efficacy of the gripper in mitigating the reaction force of the circular saw.

Moreover, Fig. 20 reveals that among 150 successful cases, seven were attributed to collisions between the cutting module and fruits or the failure to sustain the grip after cutting. Nonetheless, compared to the fruit damage rate of 8% (4 out of 50) in our previous study, these seven failures out of 150 cases reflect a notably lower damage rate of 4.7% (Park et al., 2022).

The proposed gripper allows for easy replacement of the cutting module, regardless of its function. The authors are currently working on further miniaturisation of the cutting module while determining areas for improvement. In summary, the reasons for conducting the success rate-based experiment are described below.

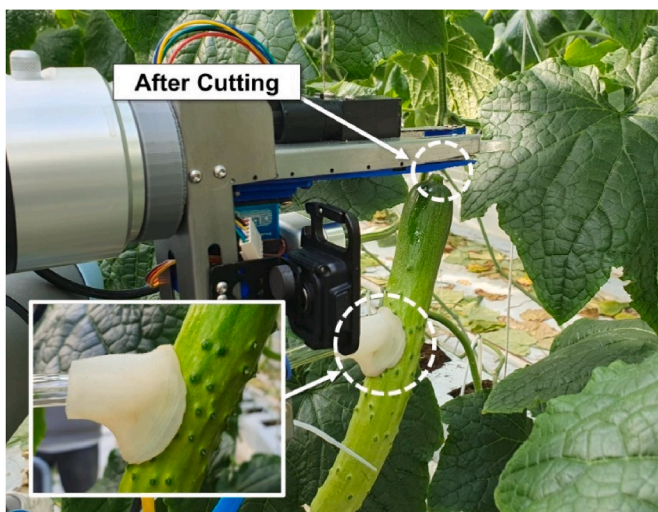


Fig. 20. In most cases, grasping remains after cutting. If the grasping is not maintained, the cucumber falls freely after cutting, colliding with the ground and damaging the cucumber.

- The performance of the proposed soft robotic gripper was indirectly confirmed by the low harvest failure rate and absence of a failure reason related to the gripper.
- Seven damaged fruits occurred through a failure to maintain grasping after harvesting and collision with the cutting module. Even if all seven cases are assumed to be grasping failures, the failure rate of 4.7% is low compared to 8% in our previous study.

However, the correlation between grasping and cutting must be verified. A fruit model called 'fruit phantom' can be used as a testbed to determine the correlation between grasping and cutting (Goulart et al., 2023a, 2023b). As a future study, the authors aim to construct an experiment to prove the hypothesis that stable grasping is helpful in performing stable cutting.

## 5. Conclusions

This research proposes a suction cup-based soft robotic gripper for cucumber harvesting. The proposed gripper adjusts the critical parameters of the shape and surface to respond to the surface and shape characteristics of cucumbers. The shape was adjusted to allow adsorption on the large curvature of the cucumber shape, maximising the effective radius representing the grasping force. In addition, the suction cup surface was adjusted to maintain adsorption on the uneven surface of the cucumber. The validity of each key parameter was verified through the test of suction cup. The experimental results reveal an increase in the grasping success rate of 100% through shape adjustment and an increase in the effective radius of 35.6% through surface adjustment. The proposed gripper is valid for cucumbers and produces strong adsorption. The proposed gripper is a subitem of the end-effector for cucumber harvesting; thus, it was integrated with the cutting module and evaluated in the field.

For rigorous evaluation, the cutting success rate was measured at three sites exhibiting different cucumber characteristics. The test of end-effector was conducted 174 times, with a harvest success rate of 86.2%, and a damage rate of 4.7%. Due to the differences in cucumber growth, the success rate of Site A was the lowest at 76.8%, and Site C was the highest at 95.2%. The analysis of the cucumber growth characteristics of each site indicates that the failure of the cutting module to cut is strongly related to the thickness and length of the cucumber pedicel.

The grasping module proposed by the authors has a function independent of the cutting module, and there is no performance degradation in replacing the cutting module. Thus, the proposed gripping module can contribute to effective cucumber harvesting if the cutting module is replaced. This analysis motivates the improvement of the cutting module of small size and better cutting performance. Additionally, experiments on the relationship between grasping and cutting are currently in



progress, and these experiments are performed by adjusting the voltage of the vacuum pump on the testbed which consists of hanging fruit phantom. In the future, this research will contribute to constructing an autonomous cucumber harvesting robot.

## Declaration of competing interest

The authors declare that they have no known competing financial interests or personal relationships that could have appeared to influence the work reported in this paper.

## Acknowledgment

This work was supported by the National Research Foundation of Korea (NRF) grant funded by the Korea government (MSIT) (No. NRF-2023R1A2C1003701).

## References

- Alian, A., Zareinejad, M., & Talebi, H. A. (2023). Curvature tracking of a two-segmented soft finger using an adaptive sliding-mode controller. *IEEE/ASME Transactions on Mechatronics*, 28, 50–59. <https://doi.org/10.1109/TMECH.2022.3210030>
- Aoyama, H., Wang, Z., & Hirai, S. (2022). Shell gripper inspired by human finger structure for automatically packaging agricultural product. In *2022 IEEE-RAS 21st international conference on humanoid robots (humanoids)* (pp. 90–95). IEEE. <https://doi.org/10.1109/Humanoids53995.2022.10000125>.
- Barbedo, J. G. A. (2016). A review on the main challenges in automatic plant disease identification based on visible range images. *Biosystems Engineering*, 144, 52–60. <https://doi.org/10.1016/j.biosystemseng.2016.01.017>
- Blanes, C., Ortiz, C., Mellado, M., & Beltrán, P. (2015). Assessment of eggplant firmness with accelerometers on a pneumatic robot gripper. *Computers and Electronics in Agriculture*, 113, 44–50. <https://doi.org/10.1016/j.compag.2015.01.013>
- Cao, X., Zou, X., Jia, C., Chen, M., & Zeng, Z. (2019). Rrt-based path planning for an intelligent litchi-picking manipulator. *Computers and Electronics in Agriculture*, 156, 105–118. <https://doi.org/10.1016/j.compag.2018.10.031>
- Cortés, V., Blanes, C., Blasco, J., Ortiz, C., Aleixos, N., Mellado, M., Cubero, S., & Talens, P. (2017). Integration of simultaneous tactile sensing and visible and near-infrared reflectance spectroscopy in a robot gripper for mango quality assessment. *Biosystems Engineering*, 162, 112–123. <https://doi.org/10.1016/j.biosystemseng.2017.08.005>
- Fontanelli, G. A., Paduano, G., Caccavale, R., Arpent, P., Lippello, V., Villani, L., & Siciliano, B. (2020). A reconfigurable gripper for robotic autonomous depalletizing in supermarket logistics. *IEEE Robotics and Automation Letters*, 5, 4612–4617. <https://doi.org/10.1109/LRA.2020.3003283>
- Gilday, K., Lilley, J., & Iida, F. (2020). Suction cup based on particle jamming and its performance comparison in various fruit handling tasks. In *2020 IEEE/ASME international conference on advanced intelligent mechatronics (AIM)* (pp. 607–612). IEEE. <https://doi.org/10.1109/AIM43001.2020.9158945>.
- Goulart, R., Jarvis, D., & Walsh, K. B. (2023a). Evaluation of end effectors for robotic harvesting of mango fruit. *Sustainability*, 15, 6769. <https://doi.org/10.3390/su15086769>
- Goulart, R., Jarvis, D., & Walsh, K. B. (2023b). Fruit phantoms for robotic harvesting trials—mango example. *Sustainability*, 15, 1789. <https://doi.org/10.3390/su15031789>
- Guo, M., Wu, P., Yi, B., Gealy, D., McKinley, S., & Abbeel, P. (2019). Blue gripper: A robust, low-cost, and force-controlled robot hand. In *2019 IEEE 15th international conference on automation science and engineering (CASE)* (pp. 1505–1510). IEEE. <https://doi.org/10.1109/COASE.2019.8843134>.
- Han, F., Fei, L., Zou, R., Li, W., Zhou, J., & Zhao, H. (2023). A restorable, variable stiffness pneumatic soft gripper based on jamming of strings of beads. *IEEE Transactions on Robotics*. <https://doi.org/10.1109/TRO.2023.3280595>
- Hayashi, S., Takahashi, K., Yamamoto, S., Saito, S., & Komeda, T. (2011). Gentle handling of strawberries using a suction device. *Biosystems Engineering*, 109, 348–356. <https://doi.org/10.1016/j.biosystemseng.2011.04.014>
- Horgan, C. O., & Saccomandi, G. (1999). Simple torsion of isotropic, hyperelastic, incompressible materials with limiting chain extensibility. *Journal of Elasticity*, 56, 159–170.
- Hudoklin, J., Seo, S., Kang, M., Seong, H., Luong, A. T., & Moon, H. (2022). Vacuum suction cup modeling for evaluation of sealing and real-time simulation. *IEEE Robotics and Automation Letters*, 7, 3616–3623. <https://doi.org/10.1109/LRA.2022.3145509>
- Jang, N., Lee, M. W., & Hwang, D. (2021). A suction-based peripheral nerve gripper capable of controlling the suction force. *IEEE/ASME Transactions on Mechatronics*, 26, 1867–1876. <https://doi.org/10.1109/TMECH.2021.3077078>
- Jun, J., Kim, J., Seol, J., Kim, J., & Son, H. I. (2021). Towards an efficient tomato harvesting robot: 3d perception, manipulation, and end-effector. *IEEE Access*, 9, 17631–17640. <https://doi.org/10.1109/ACCESS.2021.3052240>
- Lange, F., Pfanne, M., Steinmetz, F., Wolf, S., & Stulp, F. (2021). Friction estimation for tendon-driven robotic hands. In *2021 IEEE international conference on robotics and automation (ICRA)* (pp. 6505–6511). IEEE. <https://doi.org/10.1109/ICRA48506.2021.9560964>.
- Lee, J. Y., Seo, Y. S., Park, C., Koh, J. S., Kim, U., Park, J., Rodrigue, H., Kim, B., & Song, S. H. (2020a). Shape-adaptive universal soft parallel gripper for delicate grasping using a stiffness-variable composite structure. *IEEE Transactions on Industrial Electronics*, 68, 12441–12451. <https://doi.org/10.1109/TIE.2020.3044811>
- Lee, K., Wang, Y., & Zheng, C. (2020b). Twister hand: Underactuated robotic gripper inspired by origami twisted tower. *IEEE Transactions on Robotics*, 36, 488–500. <https://doi.org/10.1109/TRO.2019.2956870>
- Li, Z., Li, P., Yang, H., & Wang, Y. (2013). Stability tests of two-finger tomato grasping for harvesting robots. *Biosystems Engineering*, 116, 163–170. <https://doi.org/10.1016/j.biosystemseng.2013.07.017>
- Li, S., Stampfli, J. J., Xu, H. J., Malkin, E., Diaz, E. V., Rus, D., & Wood, R. J. (2019). A vacuum-driven origami “magic-ball” soft gripper. In *2019 international conference on robotics and automation (ICRA)* (pp. 7401–7408). IEEE. <https://doi.org/10.1109/ICRA.2019.8794068>.
- Lindenroth, L., Stoyanov, D., Rhode, K., & Liu, H. (2023). Toward intrinsic force sensing and control in parallel soft robots. *IEEE/ASME Transactions on Mechatronics*, 28, 80–91. <https://doi.org/10.1109/TMECH.2022.3210065>
- Liu, S., Zhu, Y., Zhang, Z., Fang, Z., Tan, J., Peng, J., Song, C., Asada, H. H., & Wang, Z. (2020). Otariidae-inspired soft-robotic supernumerary flippers by fabric kirigami and origami. *IEEE/ASME Transactions on Mechatronics*, 26, 2747–2757. <https://doi.org/10.1109/TMECH.2020.3045476>
- Low, J. H., Khin, P. M., Han, Q. Q., Yao, H., Teoh, Y. S., Zeng, Y., Li, S., Liu, J., Liu, Z., y Alvarado, P. V., et al. (2021). Sensorized reconfigurable soft robotic gripper system for automated food handling. *IEEE/ASME Transactions on Mechatronics*, 27, 3232–3243. <https://doi.org/10.1109/TMECH.2021.3110277>
- Lubbers, M., van Voorst, J., Jongeneel, M., & Saccon, A. (2022). Learning suction cup dynamics from motion capture: Accurate prediction of an object’s vertical motion during release. In *2022 IEEE/RSJ international conference on intelligent robots and systems (IROS)* (pp. 1541–1547). IEEE. <https://doi.org/10.1109/IROS47612.2022.9982211>.
- Mahlein, A. K. (2016). Plant disease detection by imaging sensors—parallels and specific demands for precision agriculture and plant phenotyping. *Plant Disease*, 100, 241–251. <https://doi.org/10.1094/PDIS-03-15-0340-FE>
- Navas, E., Fernández, R., Sepúlveda, D., Armada, M., & Gonzalez-de Santos, P. (2021). Soft gripper for robotic harvesting in precision agriculture applications. In *2021 IEEE international conference on autonomous robot systems and competitions (ICARSC)* (pp. 167–172). IEEE. <https://doi.org/10.1109/ICARSC52212.2021.9429797>
- Oberti, R., Marchi, M., Tirelli, P., Calcante, A., Iriti, M., Tona, E., Hocevar, M., Baur, J., Pfaff, J., Schütz, C., et al. (2016). Selective spraying of grapevines for disease control using a modular agricultural robot. *Biosystems Engineering*, 146, 203–215. <https://doi.org/10.1016/j.biosystemseng.2015.12.004>
- Orzali, L., Corsi, B., Forni, C., Riccioni, L., et al. (2017). Chitosan in agriculture: A new challenge for managing plant disease. *Biological activities and application of marine polysaccharides*, 17–36.
- Park, Y., Seol, J., Pak, J., Jo, Y., Jun, J., & Son, H. I. (2022). A novel end-effector for a fruit and vegetable harvesting robot: Mechanism and field experiment. *Precision Agriculture*, 1–23. <https://doi.org/10.1007/s11119-022-09981-5>
- Park, Y., Seol, J., Pak, J., Jo, Y., Kim, C., & Son, H. I. (2023). Human-centered approach for an efficient cucumber harvesting robot system: Harvest ordering, visual servoing, and end-effector. *Computers and Electronics in Agriculture*, 212, 108116. <https://doi.org/10.1016/j.compag.2023.108116>
- Rahman, N., Caldwell, D., & Cannella, F. (2018). Varo-fi: A variable orientable gripper to obtain in-hand manipulation. In *2018 IEEE/RSJ international conference on intelligent robots and systems (IROS)* (pp. 4568–4575). IEEE. <https://doi.org/10.1109/IROS.2018.8594380>.
- Rateni, G., Cianchetti, M., Ciuti, G., Menciassi, A., & Laschi, C. (2015). Design and development of a soft robotic gripper for manipulation in minimally invasive surgery: A proof of concept. *Meccanica*, 50, 2855–2863. <https://doi.org/10.1007/s11012-015-0261-6>
- Rong, J., Wang, P., Wang, T., Hu, L., & Yuan, T. (2022). Fruit pose recognition and directional orderly grasping strategies for tomato harvesting robots. *Computers and Electronics in Agriculture*, 202, 107430. <https://doi.org/10.1016/j.compag.2022.107430>
- Shafer, A., & Deshpande, A. D. (2022). Human-like endtip stiffness modulation inspires dexterous manipulation with robotic hands. *IEEE Transactions on Neural Systems and Rehabilitation Engineering*, 30, 1138–1146. <https://doi.org/10.1109/TNSRE.2022.3167400>
- Valiollahi, A., Shojaeifard, M., & Baghani, M. (2019). Closed form solutions for large deformation of cylinders under combined extension-torsion. *International Journal of Mechanical Sciences*, 157, 336–347. <https://doi.org/10.1016/j.ijmecsci.2019.04.053>
- Wang, Z., Or, K., & Hirai, S. (2020). A dual-mode soft gripper for food packaging. *Robotics and Autonomous Systems*, 125, 103427. <https://doi.org/10.1016/j.robot.2020.103427>
- Wang, Z., Torigoe, Y., & Hirai, S. (2017). A prestressed soft gripper: Design, modeling, fabrication, and tests for food handling. *IEEE Robotics and Automation Letters*, 2, 1909–1916. <https://doi.org/10.1109/LRA.2017.2714141>
- Yang, Y., Zhu, H., Liu, J., Li, Y., Zhou, J., Ren, T., & Ren, Y. (2022). An untethered soft robotic gripper with adjustable grasping modes and force feedback. In *2022 IEEE*



- international conference on robotics and biomimetics (ROBIO) (pp. 1–6). IEEE. <https://doi.org/10.1109/ROBIO55434.2022.10011866>.
- Yue, T., Si, W., Partridge, A. J., Yang, C., Conn, A. T., Bloomfield-Gadêlha, H., & Rossiter, J. (2022). A contact-triggered adaptive soft suction cup. *IEEE Robotics and Automation Letters*, 7, 3600–3607. <https://doi.org/10.1109/LRA.2022.3147245>
- Zhu, W., Lu, C., Zheng, Q., Fang, Z., Che, H., Tang, K., Zhu, M., Liu, S., & Wang, Z. (2023). A soft-rigid hybrid gripper with lateral compliance and dexterous in-hand manipulation. *IEEE/ASME Transactions on Mechatronics*, 28, 104–115. <https://doi.org/10.1109/TMECH.2022.3195985>